



This is a repository copy of *Enhancing the seismic performance of historic timber buildings in Asia by applying super-elastic alloy to a Chinese complex bracket system* .

White Rose Research Online URL for this paper:  
<http://eprints.whiterose.ac.uk/124944/>

Version: Accepted Version

---

**Article:**

Xie, W., Araki, Y. and Chang, W.-S. [orcid.org/0000-0002-2218-001X](https://orcid.org/0000-0002-2218-001X) (2018) Enhancing the seismic performance of historic timber buildings in Asia by applying super-elastic alloy to a Chinese complex bracket system. *International Journal of Architectural Heritage: conservation, analysis, and restoration*. ISSN 1558-3058

<https://doi.org/10.1080/15583058.2018.1442528>

---

**Reuse**

Items deposited in White Rose Research Online are protected by copyright, with all rights reserved unless indicated otherwise. They may be downloaded and/or printed for private study, or other acts as permitted by national copyright laws. The publisher or other rights holders may allow further reproduction and re-use of the full text version. This is indicated by the licence information on the White Rose Research Online record for the item.

**Takedown**

If you consider content in White Rose Research Online to be in breach of UK law, please notify us by emailing [eprints@whiterose.ac.uk](mailto:eprints@whiterose.ac.uk) including the URL of the record and the reason for the withdrawal request.



[eprints@whiterose.ac.uk](mailto:eprints@whiterose.ac.uk)  
<https://eprints.whiterose.ac.uk/>

# Enhancing the Seismic Performance of Historic Timber Buildings in Asia by applying Super-Elastic Alloy to a Chinese Complex Bracket System

Wenjun Xie, Yoshikazu Araki, Wen-Shao Chang

## Abstract

Historic timber structures that are widely distributed in East Asia are suffering from the earthquakes. This research is aiming to develop a technique to enhance the seismic performance of historic timber buildings with Dou-Gon system. High strength steel bars and super-elastic alloy bars have been used instead of the conventional wood peg connection to connect the base Dou and the column. Pushover tests have been done under all loading conditions. The energy dissipation capacity and the ultimate strength of the base Dou-Gon system have been increased by this simple technique. Base Dou-Gon system with super-elastic alloy bar connection shows a better anti-seismic performance due to its constant damping behaviour and longer fatigue life. Moreover, pre-strain of the super-elastic alloy bar can give a better damping behaviour to the base Dou system.

## 1. Introduction

Historic timber buildings such as temples, palace halls, and residential houses are widely distributed in East Asia. Most of densely distributed locations of such buildings lie in the seismic belts in East Asia, and hence there is an urgent demand for implementing protection measures against earthquakes. To this end, a significant research effort has been devoted, especially from the late 1990s, to assess the seismic performance of historic timber buildings (Fang, et al., 2001a; Fang, et al., 2001b; Suzuki & Maeno, 2006; Yu, et al., 2008; Xue, et al., 2015).

One of the primary structural components of historic timber buildings is an interlocking bracket complex, shown in Figure 1, called Dou-Gon in Chinese. Dou-Gon is located on top of a column to support a beam, and it transmits the vertical load of the upper frame and the roof to the column. Dou-Gon is composed mainly of the Dou, Gong, and Ang elements. Dou is a rectangular timber element with a cross groove at its upper side. Gong and Ang are timber

elements placed onto the cross groove of Dou. The base Dou sits on the top of a column, and wood pegs are used to connect the base Dou to the column.

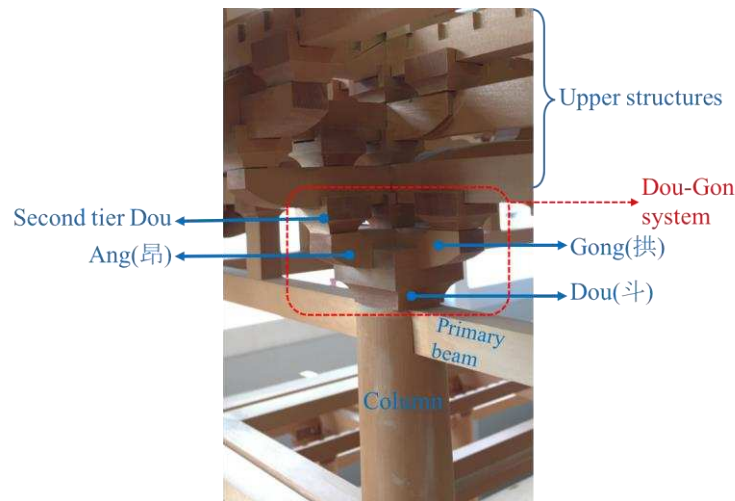


Figure 1 Details of Dou-Gon system

The nonlinear nature of the restoring force of Dou-Gon has been investigated through static and dynamic experiments (Fujita, 2000; Suzuki, 2006; Kyuke, 2008; Tsuwa, 2008; Yu, 2008; Xue, 2015; Yeo, 2016a; Yeo, 2016b) and dynamic simulations (D'Ayala, 2008; Tsai, 2011). It has been pointed out that Dou-Gon dissipates significant amount of energy mainly due to sliding between wood elements and yielding of wood elements in compression perpendicular to the grain (Fujita, 2000; Kyuke, 2008; Xue, 2015; Yeo, 2016a; Yeo, 2016b). Tsuwa et al. (2008) and Yeo et al. (2016) derived formulations for predicting the skeleton curve of the restoring force from the compression tests perpendicular to grain. D'Ayala et al. (2008) and Tsai (2011) performed nonlinear time history analysis to assess the vulnerability of historic timber buildings with the Dou-Gon system, and pointed out the necessity of improving their seismic performance.

Through such research works, the scientific knowledge has been improved significantly on the restoring force mechanism of Dou-Gon and its influence on overall response of a building. On the other hand, the research efforts have been scarcely seen on the techniques for enhancing the seismic performance of historic timber buildings with the Dou-Gon system.

Re-centring capability and energy dissipation capacity are the two fundamental characteristics that Dou-Gon system have, to give historic timber buildings good seismic performance. Re-centring capability can pull the oblique structures back to center and energy dissipate capacity will dissipate the major seismic energy. However, the conventional connectors of Dou-Gon, wood pegs, have a low ultimate strength which cause the damages of the building during

earthquakes. It is important to introduce a technique to enhance the Dou-Gon system by keeping the original re-centring capability and increasing the energy dissipation capacity and therefore to increase the ultimate strength and equivalent damping ratio of the structure.

This paper employs a simple technique to enhance the seismic performance of Dou-Gon using metal bars. With the use of metal bars, the proposed technique attempts to increase stiffness, strength, and energy dissipation of the Dou-Gon system. Static tests are performed to assess the restoring force curve of a Dou-Gon system whose base Dou is connected to the wood base using steel and super-elastic alloy (SEA, which is also been known as shape memory alloy) bars. Simple formulations are also derived for estimating the strength of the Dou-Gon system with and without the metal bars.

## 2. Methods

This study used glued laminated timber (glulam) to build a full-scale base Dou system that duplicates an ancient structure in Sichuan Province in China. Pushover tests have been performed to obtain the load-rotation curves of base Dou with different connections of conventional wood pegs, steel bars and SEA bars. The lateral loads are applied by a hydraulic jack manually. The ultimate strength and energy dissipation capacity of each test condition can be estimated to evaluate the seismic performance of the base Dou system.

### 2.1. Specimen Preparation

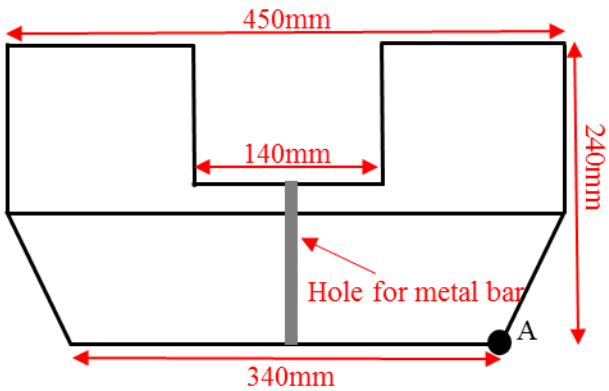
The base Dou is the Dou that sits on the top of a column in structures. In this paper, the base Dou was made by glulam of the strength class GL28h (Table 1) and its dimensions are illustrated in Figure 2. It was connected by three different materials (wood peg, high strength steel bar and SEA bar) to a timber block with the dimensions of 400x400x200mm (Figure 3). The timber block was fixed by two 24mm threaded bolts to the strong floor. One Gong and one Ang were fitted in the groove of the base Dou (Figure 4). A pallet with several wood bricks (shaded area in Figure 11) was fixed at their bottom to the top of the base element to fit the irregular top surface of the base Dou system. Several concrete blocks were pre-casted and put onto pallet to apply the vertical loads to the system.

Table 1 Mechanical properties of glulam GL28h, MPa (reference?)

Mean modulus of elasticity in bending ( $E_{0,mean}$ )	12600
Mean modulus of elasticity perpendicular to grain ( $E_{90,mean}$ )	420
Bending strength ( $f_{m,k}$ )	28

Tension strength parallel to grain ( $f_{t,0,k}$ )	19.5
Compression strength parallel to grain ( $f_{c,0,k}$ )	26.5
Compression strength perpendicular to grain ( $f_{c,90,k}$ )	3.0

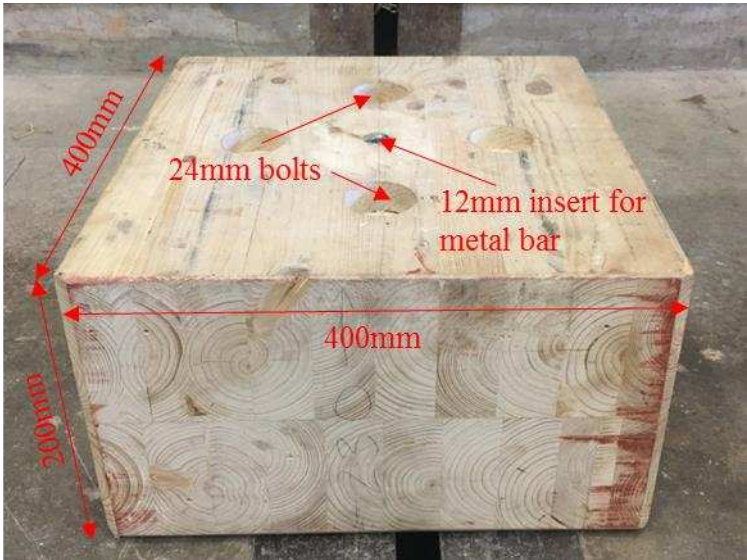
82



83

84

Figure 2 The section of base Dou



85

86

Figure 3 The timber block that fix the base Dou to the ground

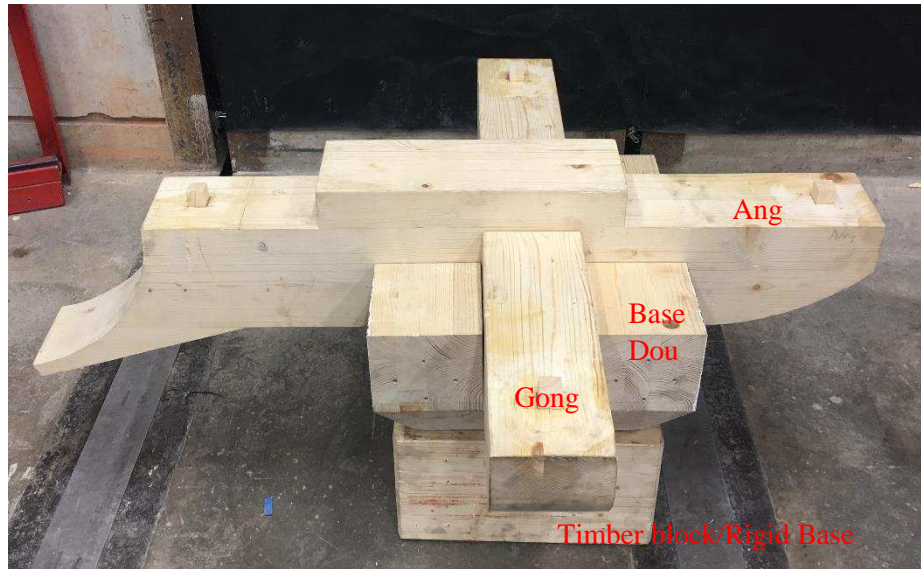


Figure 4 Dou-Gon set up without loads

A 12mm threads insert (Figure 5a) was fixed into the timber block with epoxy resin. A vertical hole was pre-drilled at the centre of the base Dou. Either high strength steel or SEA bar with threads was installed through the vertical hole of the base Dou and connected to the insert. A square steel plate with length of 100mm was embedded into the top surface of the base Dou to bear the pre-load applied to the bar and prevent damaging of the timber. A ball joint was installed at the top of the bar to remove the rotational restraint from the connection system. A nut was introduced to fix the connection system and provide pre-loading to the connection system in some cases. Details of the metal bar connecting technique can be seen from Figure 5b and 5c.

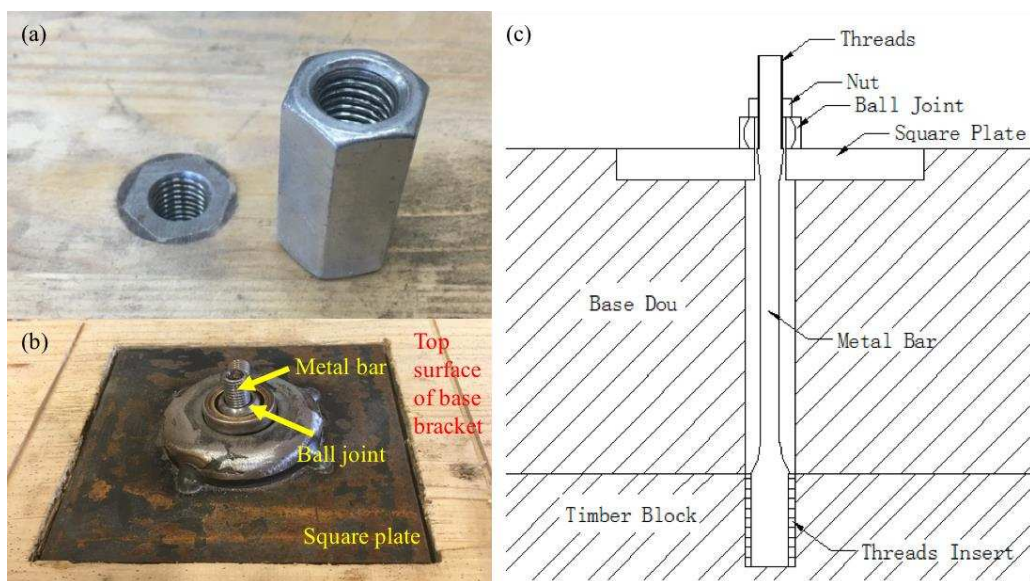


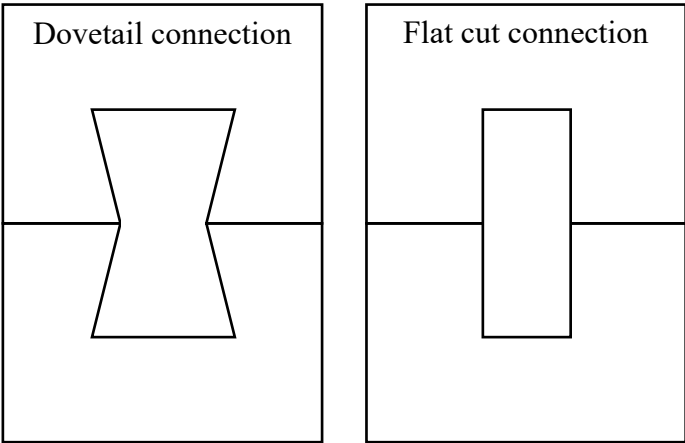
Figure 5(a) 12mm threads insert; (b) Square plate and ball joint; (c) Details of metal bar connection



100

101 **2.2. Materials for the Connection**

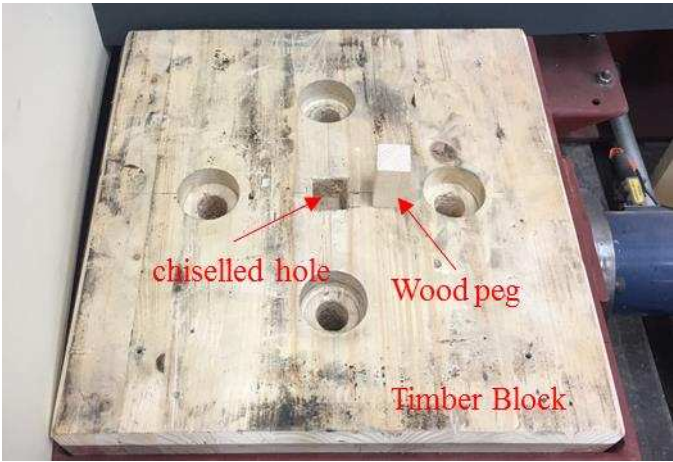
102 Wood pegs are the conventional connectors used in traditional timber structures to connect the  
103 components in the Dou-Gon system. Dovetail and flat cut (Figure 6) are the two different types  
104 of timber connections. When the connection is dovetailed, the pull out force will not be affected  
105 by the vertical load, whereas the pull out force is dependent on the vertical load with the flat  
106 cut connection (D'Ayala, 2008).



107  
108

Figure 6 Dovetail and flat cut connections

109 In this research, flat cut wood peg connection was employed. The timber grade of the peg is  
110 the same as Dou-Gon. The width of the wood pegs used in this research is one fifth of the width  
111 of the groove and the dimensions are 28x28x56mm. Cubic holes with the width of 28mm were  
112 chiselled out in both bottom of the Dou and top of the timber block respectively to install the  
113 wood peg (Figure 7).



114  
115

Figure 7 Wood peg and chiselled hole

To enhance the structural behaviour of the Dou-Gon system, the super-elastic alloy bar was employed instead of the wood peg connection. The super-elastic alloy is well-known as shape memory alloy (SMA) due to its shape memory effect. Shape memory alloy (SMA) is a metallic material with two main crystal structures, martensite and austenite which depends on temperature and external stress. The former phase is the low temperature phase whereas the latter one is the high temperature phase. There are four temperatures referring to the phase transformation,  $M_f$ ,  $M_s$ ,  $A_s$  and  $A_f$  in an ascending order.  $M_s$  and  $M_f$  are the start and finish temperature points of the martensite phase and  $A_s$  and  $A_f$  are the start and finish transformation temperatures from martensite phase back to austenite phase (Janke, et al., 2005). The shape memory effect is that crystal structure of SMA will transfer from twinned martensite to detwinned martensite by applying external stress in the temperature range of  $M_s$  and  $M_f$ . In this research, the material has super-elastic effect because the  $A_f$  of the material is much lower than the ambient temperature. The interconversion between the detwinned martensite and austenite phases will occur under loading-unloading condition. Therefore, in this paper, they have been referred to as super-elastic alloy to distinguish them from the ones with shape memory effect. The nature of SMA/SEA is schematized in Figure 8 (Chang & Araki, 2016).

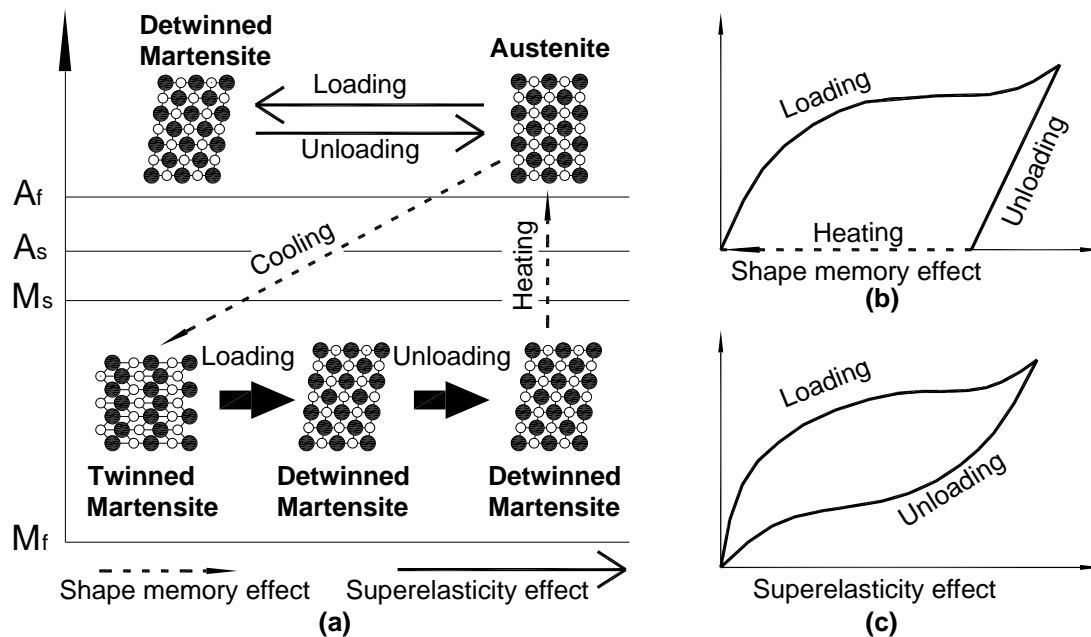


Figure 8 The different phases of SEA in different temperature, and its relation with the shape memory and superelasticity effects (Chang & Araki, 2016)

Not only the SEA bars, high strength steel bars were also used instead of the wood peg connection as a comparative parameter (Figure 9). The high strength steel bar has an ultimate tensile strength of 720MPa and SEA bar has the ultimate tensile strength of 200MPa. The SEA



used in this research have the chemical composites that measured by a Scanning Electron Microscope of copper (81.84wt%), aluminium (7.43wt%) and manganese (10.74wt%). (Araki, 2011; Omori, 2013) They are provided by Furukawa Techno Material Co., Ltd., Japan. The transformation temperature,  $A_f$ , is  $-39\text{ }^{\circ}\text{C}$ ; much lower than the normal ambient temperature that gives a stable super-elastic behaviour to the material. Both materials have an initial diameter of 12mm. The length of the specimens is 160mm. There are M8 and M12 threads at the two ends of the specimens as shown in Figure 9. The middle part of the specimens was machined down to 6mm diameter to reduce the risk that Dou will be damaged by the large pre-strain load. The length of the reduced section part is 105mm. The tensile stress-strain curves of both high strength steel bar and SEA bar are illustrated in Figure 10. The ultimate tensile strength of high strength steel bar is much higher than the SEA bar. But it was fractured at 3.6% strain. The SEA bar was pulled to 7% strain and there is negligible residual strain after unloading.

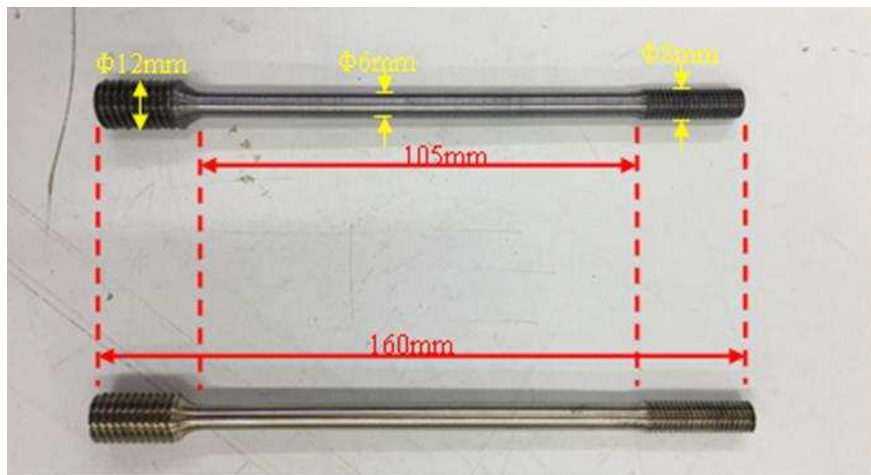


Figure 9 High strength steel bar (top) and SEA bar (bottom)

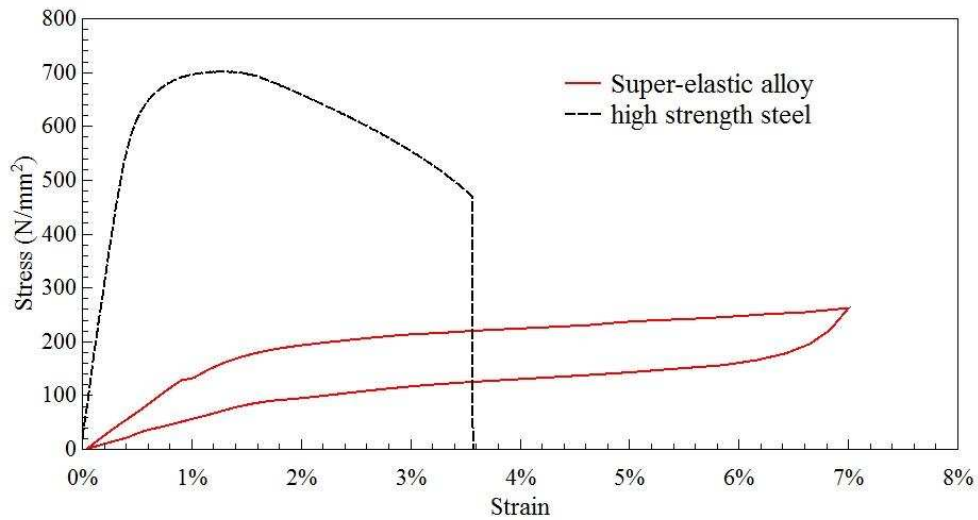


Figure 10 Stress-strain curves of metal bars

### 3. Experimental Programme

To simulate the weight of the roof supported by the Dou-Gon system, the vertical loads of three different load levels (4kN, 7kN and 10kN) were applied to the top of the specimen using concrete blocks. The specimen was rotated around point A in Figure 2 by applying a lateral load at a height of 500mm to the bottom surface of the base Dou (Figure 11) using a hydraulic jack. It recovered to its original position when the lateral load is released. The trajectory of the specimen which rotates to a certain point with prescribed radian ( $\theta$ ) and recovers to its original position is defined as one loading cycle. The specimens were tested under static cyclic loadings. Four vertical LVDTs (No 1 to 4) were used to record the rotation of the Dou and two horizontal LVDTs (No. 5 and 6) were used to record the horizontal displacement of the specimen as depicted in Figure 11. The radians ( $\theta$ ) are worked out by the differences in measurements ( $\Delta L$ ) between LVDT 1&2/3&4.

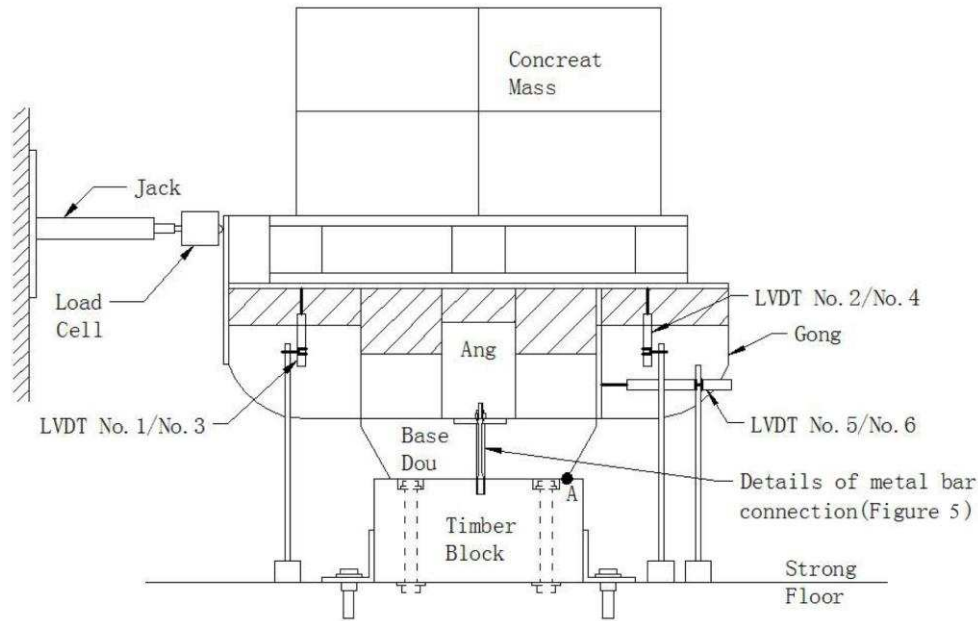


Figure 11 Loading apparatus and instrumentation used

In addition to the non-prestrain conditions, the Cu-Al-Mn SEA bars were pre-strained by stretching along the bar axis at 1%, 3% and 5% strains using a nut. The SEA bar with 1% pre-strain condition was tested under three different vertical loads 4kN, 7kN and 10kN. The SMA bar with 3% and 5% pre-strain conditions was tested under 10kN vertical load only. Table 2 lists all the test conditions.

Table 2 Experimental conditions

Vertical Loads (kN) Connector Material	4kN	7kN	10kN
Wood Peg	✓	✓	✓
High Strength Steel Bar	✓	✓	✓
SMA Bar	✓	✓	✓
SEA Bar with 1% pre-strain	✓	✓	✓
SEA Bar with 3% pre-strain			✓
SEA Bar with 5% pre-strain			✓

Generally, all specimens were rotated up to when  $\Delta L$  is 80mm with 10mm increment. The specimens with steel bar connection experienced 3 loading cycles when  $\Delta L$  equals to 60mm and was loaded 10 cycles in total. For the specimens with SEA bar connection, it was loaded 2 cycles at  $\Delta L = 70\text{mm}$  when the SEA bar has 0% pre-strain under 10kN vertical loads and only 1 loading cycle for each prescribed rotations with other SEA bar connection conditions. The specimens with wood peg connections were tested for only one loading cycle with  $\theta = 10\%$ . The actual setup can be seen in Figure 12.

Table 3 Loading conditions

$\Delta L(\text{mm})$	High Strength Steel Bar Connections	SEA Bar Connection with 0% pre-strain under 10kN vertical load	Other SEA Bar Connections
10	1 cycle	1 cycle	1 cycle
20	1 cycle	1 cycle	1 cycle
30	1 cycle	1 cycle	1 cycle
40	1 cycle	1 cycle	1 cycle
50	1 cycle	1 cycle	1 cycle
60	3 cycles	1 cycle	1 cycle
70	1 cycle	2 cycles	1 cycle
80	1 cycle	1 cycle	1 cycle



Figure 12 The test setup of Dou-Gon with 10kN dead load

## 4. Results and discussions

### 4.1. Base Dou system with conventional wood peg connector

The specimens with wood peg connectors have been tested for one loading cycle with  $\theta=10\%$ . The hysteresis loops (Figure 13) illustrated the non-linear restoring force of the Dou-Gon system with conventional wood peg connector. Three stages of stiffness could be discovered from the hysteresis loops, the elastic, plastic and limit stages (Yu, 2008). The elastic stage has a high stiffness which is independent of the vertical loads. The applied lateral load increases rapidly until reaching the yield point. At the plastic stage, the wood peg connection began to bear the shear and flexural moments and was pulled out from the chiselled hole as the lateral load increased to reach the limit rotation. The ultimate strength and the second stiffness of the base Dou system increased significantly with the vertical loads. Higher vertical loads made a

greater contribution to the P-Delta effect which results in a lower limit stiffness of the base  
 Dou system. The restoring force of the structure with wood peg connection can be calculated  
 as:

$$F = \frac{P \times \cos \theta}{L \times H} (aL - 2a^2 - 2ah \times \tan \theta - \frac{h^2 \times \tan^2 \theta}{2}) \quad (1)$$

where  $P$  is the vertical load,  $L$ ,  $H$ ,  $a$  and  $h$  are illustrated in

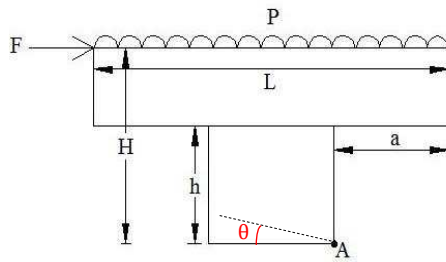


Figure 14.

The equation also expresses that the restoring force will increase with increasing the vertical  
 load applied on the top of the Dou-Gon system. The restoring force curve obtained using the  
 restoring force model is shown in Figure 13 when the vertical load is 10kN.

The energy dissipation is the energy loss per loading cycle which is represented by area  
 enclosed by each hysteresis loop. The energy dissipation of Dou-Gon with a wood peg  
 connection (Table 4) has a significant rise when the vertical loads increased from 4kN to 7kN  
 and remain constant when the vertical loads reached 10kN. The base Dou system with  
 conventional wood peg connection shows a full re-centring capability as expected because the  
 system came back to its original position without any sliding after unloading.

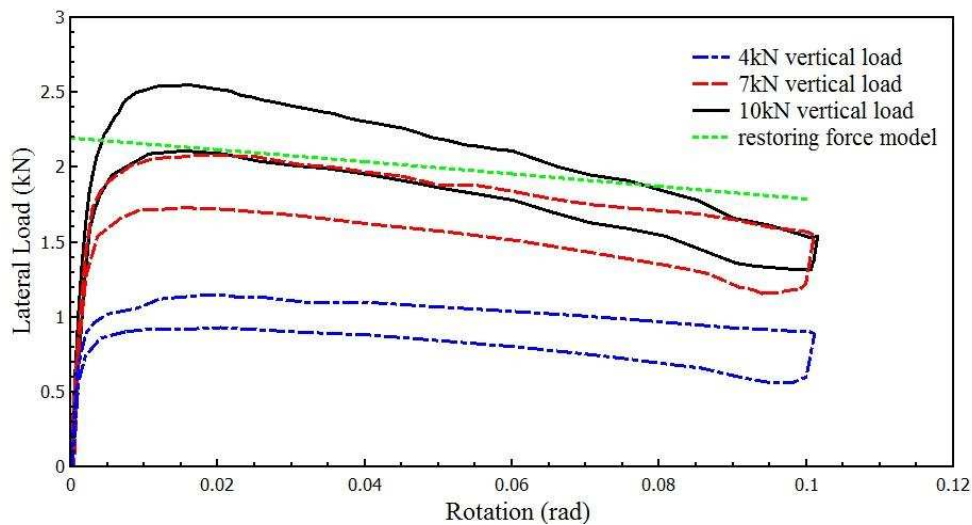


Figure 13 The first cycle hysteresis loop of Dou-Gon with wood peg connection

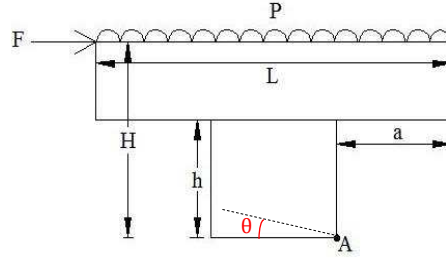


Figure 14 Simplified model of the structure and loadings

Table 4 The energy dissipation of Dou-Gon system with a wood peg connection

Vertical Loads (kN)	4	7	10
Energy dissipation (N.rad)	23.8	34.7	34.9

## 4.2. Behaviour of base Dou system with different vertical connectors

The hysteresis loops of the Dou-Gon system with connectors made of 3 different materials and under 3 different vertical loads are illustrated in Figure 15 to Figure 17. The figures clearly show that the Dou-Gon itself already has a good re-centering capability with wood peg connector and the re-centring force was given by the vertical loads representing the heavy roof weight. Such re-centering characteristics are also seen in the literature (Suzuki, 2006; Yu, 2008).

The base Dou system with SEA bar connection has experienced four stages stiffness. The first two stiffness are the stiffness of the timber structure since there was little gap between the structure and the connection system. The lateral load needs to overcome the vertical loads until the SEA bar starts to work. So, the third and fourth stiffness are the stiffness of the entire system. The restoring force curves reproduce the base Dou system with SEA bar connection and showed a good matching with the experimental results for 4kN and 7kN dead load levels, while a yield load higher than the experimental yield force was observed for the 10kN dead load. The restoring force of the structure with SEA bar connection can be calculated as:

$$F = \frac{P \times \cos \theta}{L \times H} \left( aL - 2a^2 - 2ah \times \tan \theta - \frac{h^2 \times \tan^2 \theta}{2} \right) + \frac{k_1 \left( \frac{L}{2} - a \right)^2 \sin \theta}{H} \quad (2)$$

when  $\theta \leq 0.59\%$ ;

$$F = \frac{P \times \cos \theta}{L \times H} \left( aL - 2a^2 - 2ah \times \tan \theta - \frac{h^2 \times \tan^2 \theta}{2} \right) + \frac{k_2 \left( \frac{L}{2} - a \right)^2 \sin \theta + A \left( \frac{L}{2} + a \right)}{H} \quad (3)$$

when  $\theta > 0.59\%$ .  $k_1$  and  $k_2$  are the tensile stiffness of SEA bar.



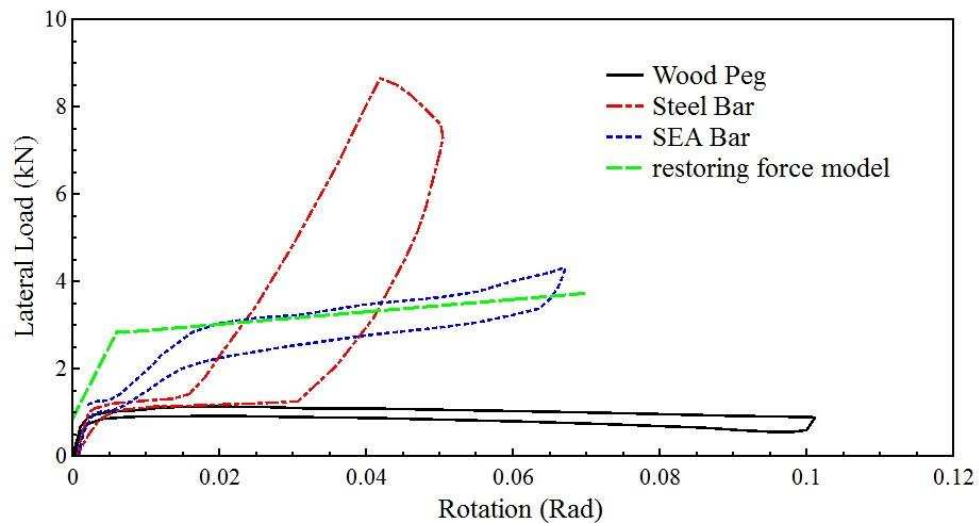


Figure 15 The second cycle hysteresis loops of Dou-Gon under 4kN dead load

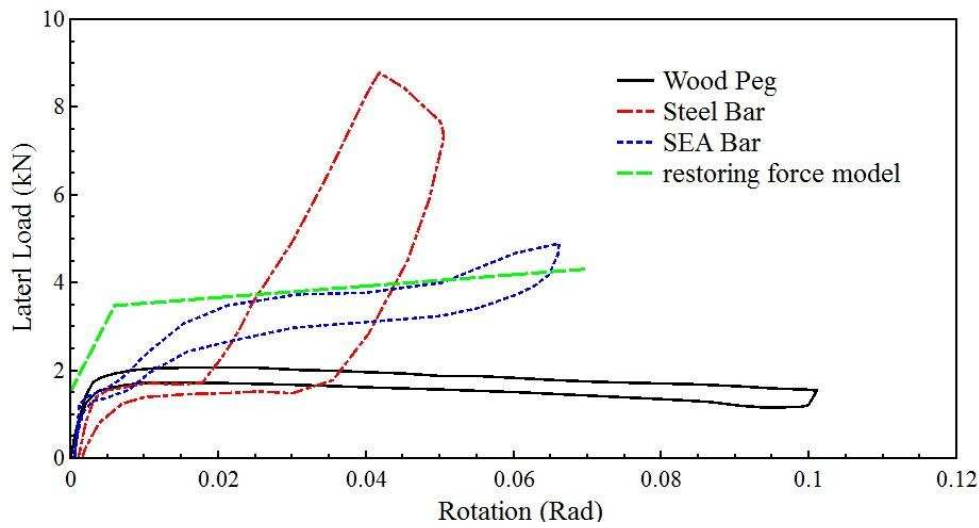


Figure 16 The second cycle hysteresis loops of Dou-Gon under 7kN dead load

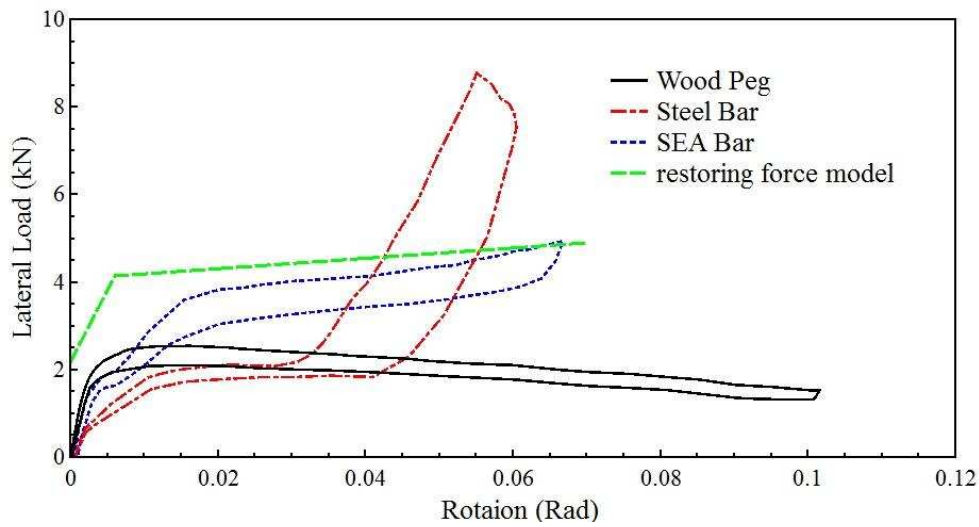


Figure 17 The second cycle hysteresis loops of Dou-Gon under 10kN dead load

In general, the base Dou system with a high strength steel bar connection has a higher ultimate strength than those with wood peg or SEA bar connectors, and it has greater secant stiffness as well. The reason for the atypical shape of base Dou system with high strength steel bar connection are illustrated in Figure 18a. The high strength steel bar connection dissipated more energy than SEA bar connection in the first loading cycle. However, in the second loading cycle, before the Dou-Gon with high strength steel connection reaches the ultimate strength, it needs to undergo a stage with very low tangent stiffness because the steel bar has already experienced several loading cycles with smaller rotational angle. The low stiffness comes from the structure itself. The high strength steel bar has permanent deformations and with low stiffness after first loading cycle called pinching effect. The energy dissipation of SEA bar connection has negligible difference between the first two loading cycles. The Dou-Gon with high strength steel bar connection was subjected to 3 loading cycles at  $\Delta L = 60\text{mm}$ . The areas in the hysteresis loops significantly reduced during the 2<sup>nd</sup> and 3<sup>rd</sup> loading cycles (Figure 19). The high strength steel bar fractured before the specimen reached  $\Delta L = 80\text{mm}$ . On the other hand, 2 loading cycles were applied to the Dou-Gon system with SEA bar connection at  $\Delta L = 70\text{mm}$ . During the loading cycles, the shape of hysteresis loops almost remains unchanged (Figure 19).

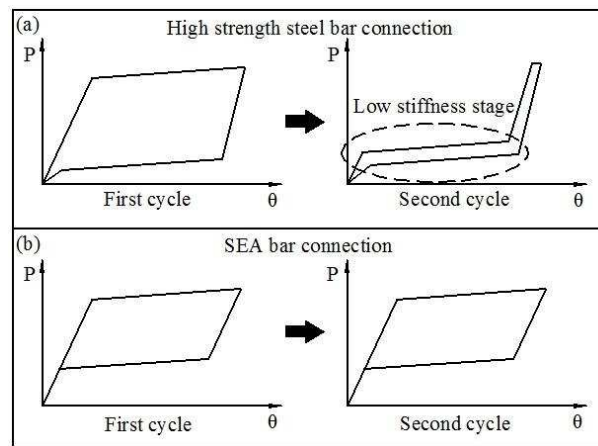


Figure 18 Schematic illustration of first two loadings cycles of Dou-Gon connects by (a) high strength steel bar and (b) SMA bar

Equivalent damping ratios ( $\zeta$ ) for each loading case were calculated by equation:

$$\zeta = \frac{A_h}{4\pi \times A_e} \quad (4)$$

where  $A_h$  is the dissipated energy in 1 loading cycle and  $A_e$  is the maximum elastic strain energy in 1 loading cycle.

The equivalent damping ratio of high strength steel bar connection when  $\Delta L=70\text{mm}$  dropped from 6.35% to 2.66% and 1.40% at the 2nd and 3rd loading cycles, respectively. The SEA bar connection gave 4.13% and 4.08% equivalent damping ratios during the 2 loading cycles at  $\Delta L=70\text{mm}$  as shown in Figure 20. The high strength steel bar connection can only provide high equivalent damping ratio in the first loading cycle and fractured after few loading cycles. The SEA bar connection can give a consistent equivalent damping ratio and better fracture behaviour since there is no fracture has been gathered during the non-prestrain tests.

The high strength steel bar connection has permanent deformation after each loading cycle, which reduces damping capacity while the SMA bar connection gives a consistent damping behaviour to the Dou-Gon system. Several aftershocks happen after the main shock in an earthquake. This requires the Dou-Gon system has stable damping ratio to dissipate energy during the aftershocks as well. The high strength steel bar connections provide low equivalent damping ratio and small resistance to the Dou-Gon during the aftershocks since they would have permanent deformations after the main shock. And the SEA bar connections can give consistent damping behaviour and dissipate energy persistent in both main shock and aftershocks.

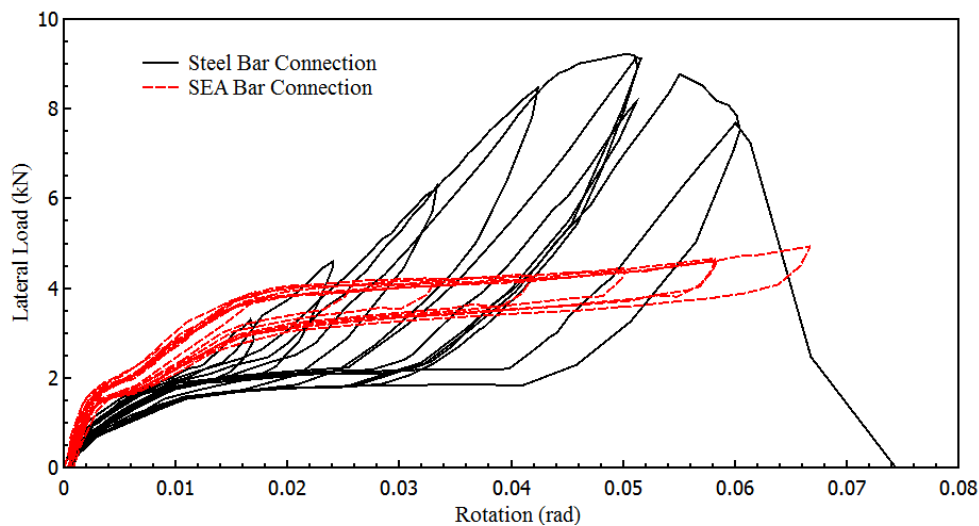


Figure 19 Hysteresis loop histories of both high strength steel bar and SMA bar connections under 10kN vertical loads

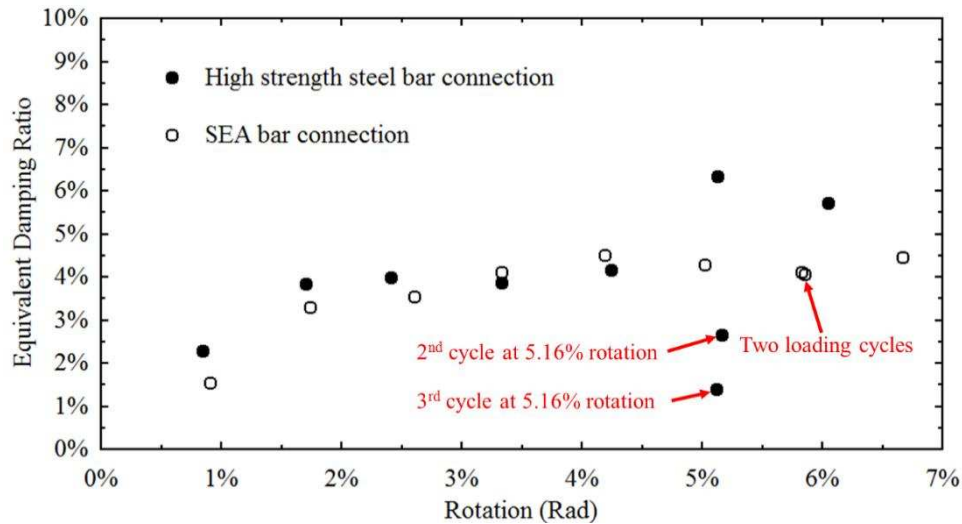


Figure 20 Equivalent damping ratios of both high strength steel bar and SMA bar connections under 10kN vertical loads

### 4.3. The effects of SMA bar connector with different levels of pre-strain

Previous research works showed that the pre-strain of SEA bars will give to the materials a larger energy dissipation capacity. In this research, the SEA bar connections was pre-strained to 1%, 3% and 5% strain levels, aiming at a higher damping ratio of the base Dou system.

Figure 21 illustrates that the SEA bar connector without pre-strain has experienced three stages of stiffness variation before the SEA enters the martensitic phase. So, it can only dissipate little amount of energy during small rotations. The shape of hysteresis loop of SEA bar with 1% pre-strain was not too much different from the one without pre-strain but change to the martensitic phase quicker. Because the pre-strain eliminates any possible slack between the structure and the connection system, and SEA bar starts to work from the beginning of loading. The ultimate strength increased with the increase of the pre-strain level. The lateral load started to rise again after 4.5% radians for the SEA bar connection with 3% pre-strain. Because the SEA material is at its martensitic phase when it was pre-strained to 5% strain level. The second stiffness of SEA bar connection with 5% pre-strain is much higher than others and the lateral load increased to nearly 7kN when  $\Delta L=70\text{mm}$  which gives a much better damping capacity than others. However, the SEA bar with 5% pre-strain fractured when the structure tried to reach 80mm in  $\Delta L$ .

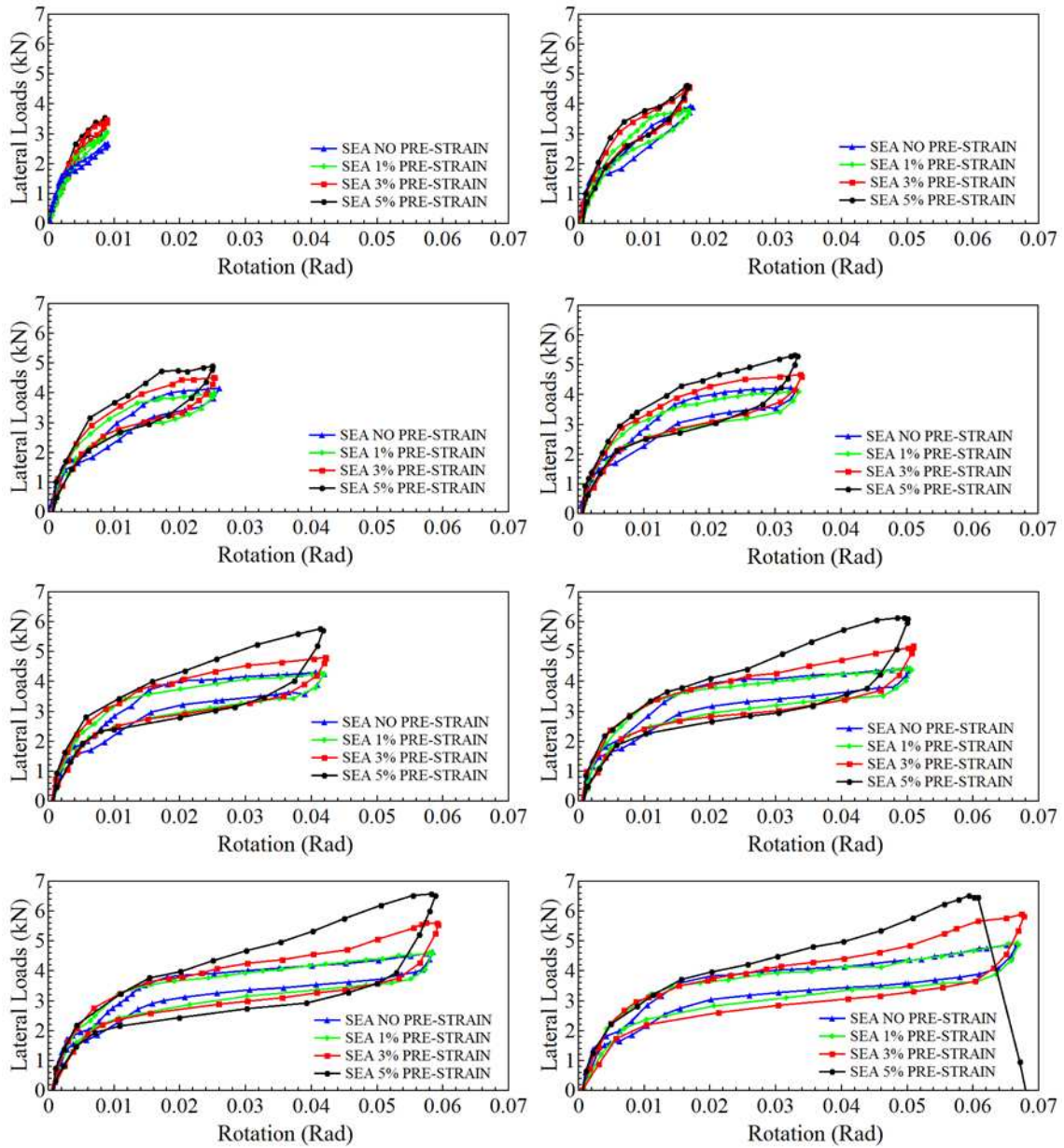


Figure 21 The hysteresis loops of Dou-Gon with SEA bar connection under 10kN dead load

Figure 22 and Figure 23 show that, under 4 and 7 kN vertical loads, SEA bar connectors with 1% pre-strain gave higher equivalent damping ratio than non-prestrain ones during small prescribed rotation and become closer when  $\theta$  increases. The equivalent damping ratio of high strength steel bar connector increases with the increasing of  $\Delta L$  and SEA bar connector gives a constant equivalent damping ratio when  $\Delta L \geq 20\text{mm}$ . The SEA bar connector with 1% pre-strain have slightly larger equivalent damping ratio than the one without pre-strain. When  $\Delta L < 40\text{mm}$ , the high strength steel bar connector has a higher equivalent damping ratio than the SEA bar connector without pre-strain but lower than the SEA bar connector with 1% pre-strain. They have the similar equivalent damping ratio when  $\Delta L = 40\text{mm}$ . Under  $\Delta L$  equals to 50mm

and 60mm, the high strength steel bar connection gives much higher equivalent damping ratios than other two connectors, but there are dramatic declines after the first cycle. The fracture strain of the high strength steel bar was tested to be  $3.7 \times 10^4 \mu\epsilon$ . The high strength steel bar connections fractured when the base Dou system trying to reach 70mm of  $\Delta L$  in both loading conditions. The behaviour was almost the same with 10kN vertical loads. No fracture happens to the SEA bars during the tests under 4kN and 7kN vertical loads which shows a longer fatigue life than high strength steel bar.

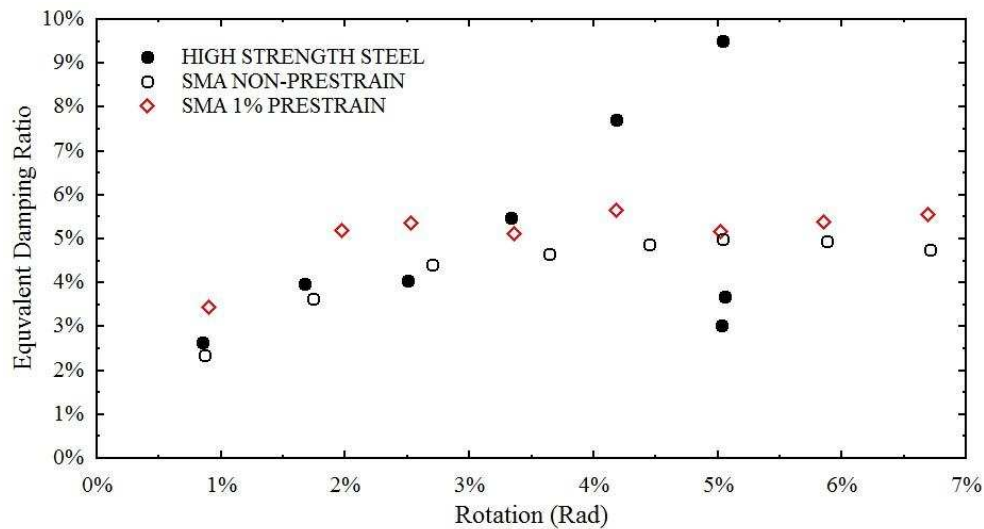


Figure 22 Equivalent damping ratios of Dou-Gon under 4kN dead loads

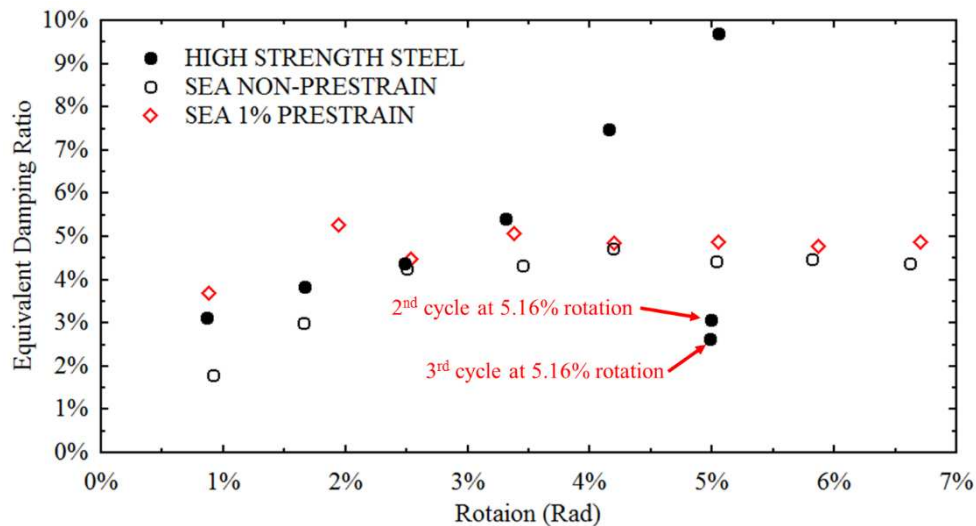


Figure 23 Equivalent damping ratios of Dou-Gon under 7kN dead loads

Under 10kN vertical loads, Figure 24, the equivalent damping ratios of SEA bar connectors with pre-strain were always larger than the ones without pre-strain. The equivalent damping



ratio is increased as the pre-strain level increased. The SEA bar connector with 5% pre-strain gave the highest damping ratio under 10kN vertical loads but fractured when  $\Delta L=80\text{mm}$ . The equivalent damping ratio of SEA bar connector with 3% pre-strain increases when  $\Delta L<40\text{mm}$  and remain constant after that. The SEA bar connector with 5% pre-strain has a rapid increase when  $\Delta L<30\text{mm}$  and rise steadily after a plateau of  $\Delta L$  is between 30mm and 50mm.

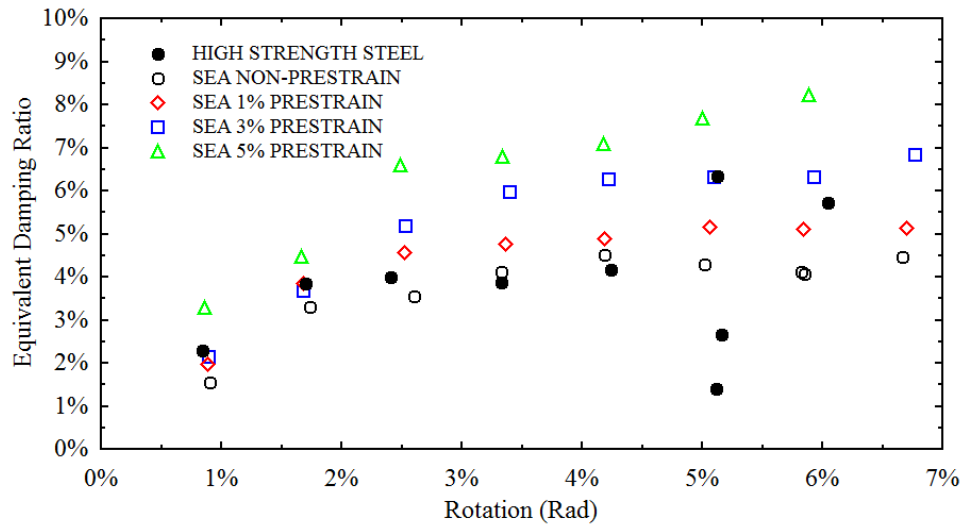


Figure 24 Equivalent damping ratios of Dou-Gon under 10kN dead loads

## 5. Conclusion

The Dou-Gon system is the primary element of the historic timber structure in Asia which is located on top of a column to transfer the upper loads to the column. The historic timber structure has expressed strong seismic performance because Dou-Gon can dissipate significant amount of energy due to sliding between wood elements and yielding of wood elements in compression perpendicular to the grain. They also have a good re-centring capability since the heavy roof gives the re-centring force to the Dou-Gon. However, they have still been damaged by earthquake seriously and the seismic performance of historic timber structure needs to be enhanced.

The conventional connection of the base Dou and column uses a wood peg. In this research, a technique has been developed to enhance the seismic performance of a base Dou system that duplicate an ancient structure in Sichuan Province in China by using super-elastic alloy and high strength steel bars. Pushover tests have been done to the base Dou system with three

different connectors (wood peg, high strength steel bars and SEA) under 4kN, 7kN and 10kN vertical loads.

The lateral load that applies on the base Dou system is overcoming the vertical loads when they are connected by the wood peg, so the ultimate strength of the base Dou system will increase with the weight of the roof. The high strength steel bar connection has a much higher ultimate strength than other types of connections, but only in the first loading cycle. For the second and third loading cycles, the equivalent damping ratio has a dramatic reduction. A consistent damping performance can be achieved by using the SEA bar connector. The pre-strain of the SEA bar gives a higher equivalent damping ratio to the base Dou system. The equivalent damping ratio increases with the pre-strain level of the SEA bar. When the SEA bar has been pre-strained to 5% strain level, the equivalent damping ratio reached a maximum of 8%. The SEA bar has a longer fatigue life than the high strength steel bar. In general, the energy dissipation capacity and ultimate strength of base Dou system have been increased by this simple technique. SEA bar is more suitable for using in the seismic application since the constant damping behaviour could overcome both main shock and aftershocks of the earthquake.

## References

- Araki, Y., Endo, T., Omori, T., Sutou, Y., Koetaka, Y., Kainuma, R. & Ishida, K., 2011. Potential of superelastic Cu-Al-Mn alloy bars for seismic applications. *Earthquake Engineering and Structural Dynamics*, Volume 40, pp. 107-115.
- Chang, W.-S. & Araki, Y., 2016. Use of shape-memory alloys in construction: a critical review. *Proceedings of the Institution of Civil Engineers - Civil Engineering*.
- D'Ayala, D. & Tsai, P.-H., 2008. Seismic vulnerability of historic Dieh-Dou timber structures in Taiwan. *Engineering Structures*, 30(8), pp. 2101-2113.
- Fang, D.-P., Iwasaki, S., Yu, M. H. & Shen, Q. P., 2001. Ancient Chinese timber architecture. I: Experimental study. *Journal of Structural Engineering*, 127(11), pp. 1348-1357.
- Fang, D. P., Iwasaki, S., Yu, M. H. & Shen, Q. P., 2001. Ancient Chinese Timber Architecture. II: Dynamic Characteristics. *Journal of Structural Engineering*, Nov.127(11).
- Fujita, K., Sakamoto, I., Ohashi, Y. & Kimura, M., 2000. Static and dynamic loading tests of bracket complexes used in traditional timber structures in Japan. *New Zealand, 12th World Conference on Earthquake Engineering*.
- Janke, L., Czaderski, C., Motavalli, M. & Ruth, J., 2005. Applications of shape memory alloys in civil engineering structures--Overview, limits and new ideas. *Materials and Structures*, 38(5), pp. 578-592.
- Kyuke, H., Kusunoki, T., Yamamoto, M., Minewaki, S. & Kibayashi, M., 2008. *Shaking Table Tests of 'MASUGUMI' Used in Traditional Wooden Architectures*. Miyazaki, s.n.
- Omori, T. & Kainuma, R., 2013. Alloys with long memories. *Nature*, 502(7469), pp. 42-44.

391 Omori, T., Kusama, T., Kawata, S., Ohnuma, I., Sutou, Y. Araki, Y., Ishida, K. & Kainuma, R., 2013.  
 392 Abnormal grain growth induced by cyclic heat treatment. *Science*, Volume 341, pp. 1500-1502.

393 Suzuki, Y. & Maeno, M., 2006. Structural mechanism of traditional wooden frames by dynamic and  
 394 static tests. *Structural Control and Health Monitoring*, Volume 13, pp. 508-522.

395 Tsai, P.-H. & D'Ayala, D., 2011. Performance-based seismic assessment method for Taiwanese  
 396 historic Dieh-Dou timber structures. *Earthquake Engineering and Structural Dynamics*, Volume 40,  
 397 pp. 709-729.

398 Tsuwa, I., Koshihara, M., Fujita, K. & Sakamoto, I., 2008. A Study on the Size Effect of Bracket  
 399 Complexes Used in Traditional Timber Structures on the Vibration Characteristics. *Miyazaki, s.n.*,  
 400 pp. 1344-1351.

401 Xue, J., Wu, Z., Zhang, F. & Zhao, H., 2015. Seismic Damage Evaluation Model of Chinese Ancient  
 402 Timber Buildings. *Advances in Structural Engineering*, 7 Nov, 18(10), pp. 1671-1683.

403 Yeo S.-Y., Hsu, M.-F., Komatsu, K., Chung, Y.-L. & Chang, W.-S., 2016. Shaking Table Test of the  
 404 Taiwanese Traditional Dieh-Dou Timber Frame. *International Journal of Architectural Heritage:*  
 405 *Conservation, Analysis, and Restoration* , 10(5), pp. 539-557.

406 Yeo, S.-Y., Komatsu, K., Hsu, M.-F. & Que, Z., 2016. Mechanical model for complex brackets  
 407 system of the Taiwanese traditional Dieh-Dou timber structures. *Advances in Structural Engineering*,  
 408 19(1), pp. 65-85.

409 Yu, M.-H., Oda, Y., Fang, D.-P. & Zhao, J.-H., 2008. Advances in structural mechanics of Chinese  
 410 ancient architectures. *Frontiers of Structural and Civil Engineering*, 2(1), pp. 1-25.

411